

# Tire–Road Contact Stiffness

D. Wang · A. Ueckermann · A. Schacht ·  
M. Oeser · B. Steinauer · B. N. J. Persson

Received: 22 July 2014 / Accepted: 17 September 2014 / Published online: 27 September 2014  
© Springer Science+Business Media New York 2014

**Abstract** When a rubber block is squeezed against a nominal flat but rough surface, the rubber bottom surface will penetrate into the substrate roughness profile. The relation between penetration depth  $w$  (or the average interfacial separation  $\bar{u}$ ) and the applied squeezing pressure  $p$  determines the (perpendicular) contact stiffness  $K = dp/dw = -dp/d\bar{u}$ , which is important for many applications. We have measured the relation between  $p$  and  $\bar{u}$  for a rubber block squeezed against 28 different concrete and asphalt road surfaces. We find a linear relation between  $\log p$  and  $\bar{u}$ , in agreement with theory predictions. The measured stiffness values correlate rather well with the theory prediction.

**Keyword** Contact stiffness · Surface roughness · Interfacial separation · Rubber block

## 1 Introduction

The stiffness of mechanical contacts is important for a large number of applications. For example, the tangential stiffness  $K_{\parallel}$  of a mechanical contact will influence the damping and wear (e.g., fretting wear) properties of the structure. The perpendicular stiffness  $K_{\perp}$  is important in tire applications where it will effect the tire noise (e.g., via the air-pumping

mechanism) and fluid squeeze-out at the tire–road interface for wet road surfaces. In addition, for elastic contact, it has been shown by Barber [1] (see also Ref. [2, 3]) that the perpendicular contact stiffness of a junction is proportional to the contact heat transfer coefficient and (for conducting materials) the electric contact conductance. We also note that the tangential contact stiffness is proportional to the perpendicular stiffness ( $K_{\parallel} \approx K_{\perp}(2 - 2\nu)/(2 - \nu)$ , where  $\nu$  is the Poisson ratio) (see Ref. [3]) so any theory or measurement of the perpendicular stiffness is relevant also for the tangential contact stiffness.

In this paper, we will report on an extensive study of the perpendicular stiffness between a rubber block and different road surfaces [4]. We have measured the contact stiffness for 28 road surfaces. The surface topography of the road surfaces was studied using an optical technique and the surface roughness power spectra obtained for all the surfaces. According to theory [3, 5–11, 15], the elastic contact stiffness of a junction is determined by the surface roughness power spectrum of the surfaces involved, and using this theory, we obtain good correlation between measured and calculated stiffness values. The influence of surface roughness on the contact stiffness has been studied before for silicon rubber [7, 8] and tire tread rubber [12–14], but here we present a much more extensive study to test the theory.

## 2 Theory

We present a very short summary of the theory used to analyze the experimental data [5–7]. Assume that an elastic block with a flat surface is squeezed against a rigid, randomly rough surface, see Fig. 1. We assume for simplicity frictionless contact so the rubber block can slip parallel to the surfaces. When the external load  $F$  (or pressure  $p = F/A_0$ ) vanish, the block touches the substrate only at

D. Wang · A. Ueckermann · A. Schacht · M. Oeser ·  
B. Steinauer  
Institute of Road and Traffic Engineering, RWTH Aachen  
University, 52074 Aachen, Germany

B. N. J. Persson (✉)  
PGI, FZ-Jülich, 52425 Jülich, Germany  
e-mail: b.persson@fz-juelich.de  
URL: <http://www.MultiscaleConsulting.com>

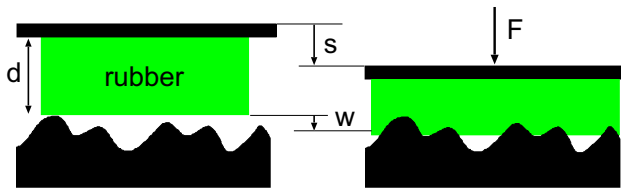


**Fig. 1** A rubber block in contact with a rigid, randomly rough substrate. *Left*: no applied load. *Right*: the rubber block is squeezed against the substrate with the force  $F$ . The upper and (the average position of) the lower surface of the rubber block moves downwards by the distances  $s$  and  $w$ , respectively. We assume perfect interfacial slip (no friction)

the top of the highest substrate asperity which has a height  $h_{\max}$  above the average substrate surface plane. Let us now increase the force  $F$ . The average plane of the bottom surface of the block will move downwards by a distance

$$w = h_{\max} - \bar{u}, \tag{1}$$

where  $\bar{u}$  denotes the average interfacial separation. In the experiment,  $w$  is not measured directly but rather the displacement  $s$  of the upper surface of the rubber block which is related to  $w$  as

$$s = w + dp/E, \tag{2}$$

where  $E$  is the Young’s modulus of the elastic solid and  $d$  the thickness of the block. In (2), the term  $dp/E$  results from the compression of the rubber block. For frictional contact (assuming no slip), one may still use (1) but the Young’s modulus must be replaced by an effective modulus  $E_{\text{eff}} > E$  which depends on the ratio  $d/D$  between the thickness  $d$  and diameter  $D$  of the elastic block [16].

In Refs. [5, 6], one of us has shown that for a wide range in the pressure  $p$  the following relation between  $p$  and the average interfacial separation  $\bar{u}$  is obeyed:

$$p = \beta E^* e^{-\bar{u}/u_0}, \tag{3}$$

where the dimensionless number  $\beta$  and the length  $u_0$  depend only on the surface roughness power spectrum. The reduced modulus  $E^* = E/(1 - \nu^2)$ . For surfaces with fractal dimension close to 2 (as is typical for road surfaces)  $u_0 \approx \gamma h_{\text{rms}}$  where  $\gamma \approx 0.4$ , where  $h_{\text{rms}}$  is the root-mean-square roughness parameter [5]. Note that  $h_{\text{rms}}$  is mainly determined by the long-wavelength roughness which is also the case for the parameters  $\beta$  and  $u_0$  in (3). Using (3), we get the normal contact stiffness

$$K = \frac{dp}{dw} = -\frac{dp}{d\bar{u}} = \frac{p}{u_0}. \tag{4}$$

We note that (3) and (4) are not valid for very small or large nominal contact pressures  $p$ . For very small contact pressure, the contact will only involve the highest substrate asperities and in this limit (which we refer to as finite size

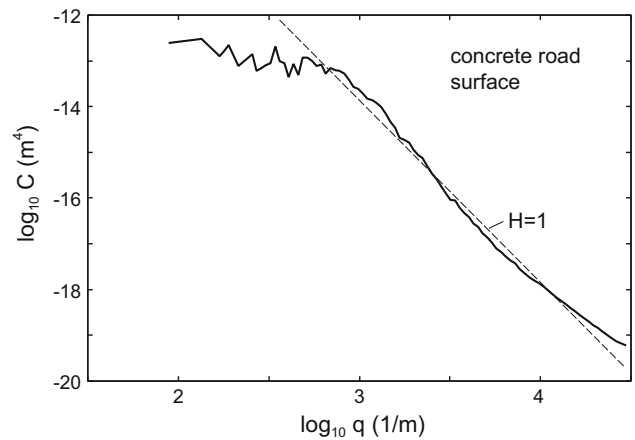


**Fig. 2** The logarithm of the surface roughness power spectrum of a concrete road surface as a function of the logarithm of the wavevector. The topography was measured over a surface area 10 cm × 10 cm. The surface has the root-mean-square (rms) roughness amplitude  $h_{\text{rms}} = 0.54$  mm and (including the roughness over the measured length scales) the rms slope 0.68. The highest and the lowest point on the studied surface area are  $h_{\max} = 1.49$  mm and  $h_{\min} = -1.73$  mm relative to the mean surface plane. The dashed line has the slope  $-4$  corresponding to a self-affine fractal surface with the Hurst exponent  $H = 1$  or fractal dimension  $D_f = 2$

pressure region), the contact will be Hertzian-like [7, 10, 17–19]. For very large pressures  $p$  nearly complete contact will occur and  $\bar{u} \approx 0$ . However, in the applications below, we are in the pressure region where (3) should be valid.

In this work, we focus mainly on the length parameter  $u_0$  which determines the contact stiffness. In Ref. [5, 6] it was shown that

$$u_0 = \sqrt{\pi\gamma} \int_{q_0}^{q_1} dq q^2 C(q) W(q), \tag{5}$$

where

$$W(q) = \left( \pi \int_{q_0}^q dq' q'^3 C(q') \right)^{-1/2},$$

where the surface roughness power spectrum [20]

$$C(q) = \frac{1}{(2\pi)^2} \int d^2x \langle h(\mathbf{x})h(\mathbf{0}) \rangle e^{-i\mathbf{q}\cdot\mathbf{x}}, \tag{6}$$

where  $h(\mathbf{x}) = h(x, y)$  is the height of the surface profile relative to the average plane. In (6)  $\langle \dots \rangle$  stands for ensemble averaging so that  $\langle h(\mathbf{x}) \rangle = 0$ . Finally, we note that the surface mean-square roughness is given by

$$h_{\text{rms}}^2 = \langle h^2(\mathbf{x}) \rangle = 2\pi \int_{q_0}^{q_1} dq q C(q) \tag{7}$$

### 3 Experimental

We have measured the relation between the displacement  $s$  and the applied nominal contact pressure  $p$  when a

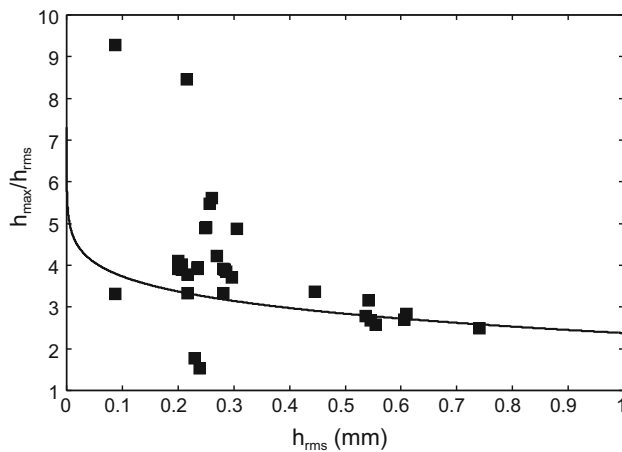


**Fig. 3** The height of the highest point (measured from the average surface plane),  $h_{\max}$ , as a function of the rms roughness amplitude  $h_{\text{rms}}$

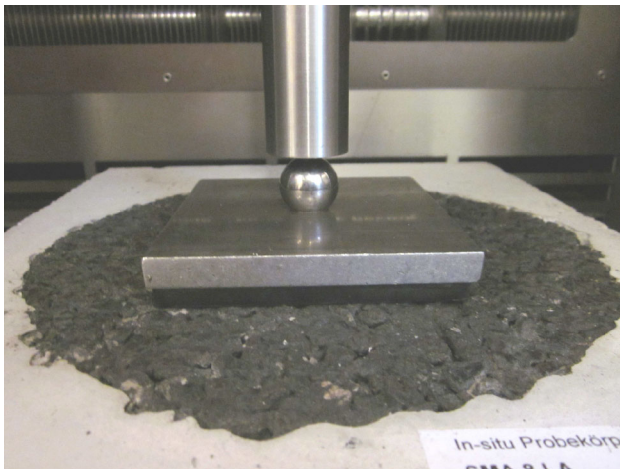


**Fig. 4** Experimental configuration for measuring the relation between the displacement  $s$  and the applied force  $F$  (or nominal contact pressure  $p = F/A_0$ )

rectangular rubber block with thickness  $d = 1$  cm and side  $L = 10$  cm is squeezed against 12 different asphalt road surfaces and 16 different concrete road surfaces. The asphalt road surfaces were drilled from road surfaces while the concrete specimens, with different roughness, grain sizes and gradation, were made in the laboratory. The surface roughness profiles of all the surfaces were obtained using an optical method which uses a chromatic white light sensor. The length parameter  $u_0$  is mainly determined by the long-wavelength roughness components, and the surfaces were therefore studied over a large area ( $10 \text{ cm} \times 10 \text{ cm}$ ) with relatively low lateral resolution ( $0.1 \text{ mm}$ ). In Fig. 2, we show the surface roughness power spectrum of one of the studied concrete surfaces. The dashed line has the slope  $-4$  corresponding to a self-affine fractal surface with the Hurst exponent  $H = 1$  or fractal dimension  $D_f = 2$ . Road surfaces usually have fractal dimension between 2.0 and 2.2 [21].

The surfaces we use have root-mean-square roughness  $h_{\text{rms}}$  from 0.087 to 0.74 mm. Figure 3 shows the height (above the average plane) of the highest asperity as a function of the rms roughness for all the studied surfaces. The solid line is the theory prediction [22]:

$$\frac{h_{\max}}{h_{\text{rms}}} \approx \left[ 2 \log \left( \frac{h_{\text{rms}} A_0}{h_{\max} \xi^2 \sqrt{(2\pi)}} \right) \right]^{1/2}$$

where  $A_0 = L^2$  and we have assumed that the surface roughness has a correlation length  $\xi \approx 10h_{\text{rms}}$  (see Appendix A in Ref. [22]).

The rubber penetration depth as a function of the applied load has been measured using a device (see Fig. 4) developed at the Institute of Road and Traffic Engineering in Aachen. The nominal contact pressure is increased linearly with time from zero to the final value 0.5 MPa in 20 s, while the vertical displacement  $s$  is registered. The force is applied to a steel plate (see Fig. 4) through a ball bearing, so the loading will result in a uniform nominal contact pressure at the rubber–road interface. The rubber block was supplied by Continental and is made from a rubber compound very similar to a tire tread compound.

The accuracy of the measurement of the nominal contact pressure is  $\pm 5$  kPa and for the displacement  $\pm 5 \mu\text{m}$ . A larger inaccuracy may prevail in the optical measurements of the surface topography, and hence in the surface roughness power spectra. One way to gain information about the accuracy of the topography data would be to perform topography measurements with other instruments, e.g., engineering stylus instrument. Optical method is usually inaccurate for the short wavelength components of the roughness profile where the surface slope may be large. This often results in a large fraction of undefined height points (about  $\approx 10\%$  in the present case). However, the contact stiffness, in the region where it is proportional to the pressure, is dominated by the long-wavelength roughness.

In order for the theory to be valid in the simple form described in Sect. 2, it is necessary that the thickness of the rubber block is larger than the diameter of the macroasperity contact regions<sup>1</sup>. This condition is satisfied even for the course-grained road surface used in Fig. 4. This is illustrated in Fig. 5 which shows pictures (system size  $10 \text{ cm} \times 10 \text{ cm}$ ) of the contact between a rubber block and two road surfaces using pressure sensitive paper (Fujifilm super low pressure LLW, pressure range between 0.5 and 2.5 MPa). The nominal contact pressure  $p = 0.5$  MPa. The fine-grained road surface (a) exhibits small (diameter  $\sim 1$  mm or less), closely spaced, macroasperity contact regions, while the course-grained surface (b) (the same

<sup>1</sup> Contact mechanics for layered materials (in this case rubber slab and rigid (steel) plate) can also be studied within the same formalism as used in deriving Eq. (3)–(5), see [23–25]

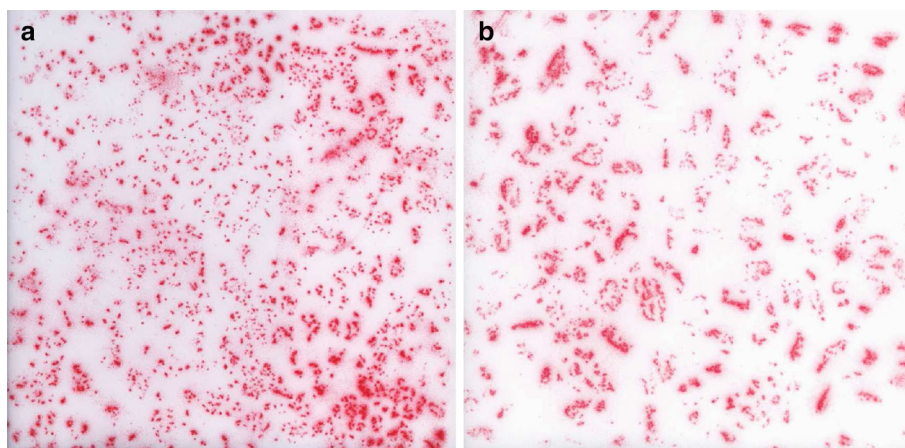


**Fig. 5** Picture of the contact between a rubber block and two road surfaces using pressure sensitive paper (system size 10 cm × 10 cm). The nominal contact pressure  $p = 0.5$  MPa. The fine-grained road surface (a) exhibit small (diameter  $\sim 1$  mm or less), closely spaced,

macroasperity contact regions, while the course-grained surface (b) (the same surface as in Fig. 4) exhibit much larger (diameter  $\sim 5$  mm or less) macroasperity contact regions with larger average separations

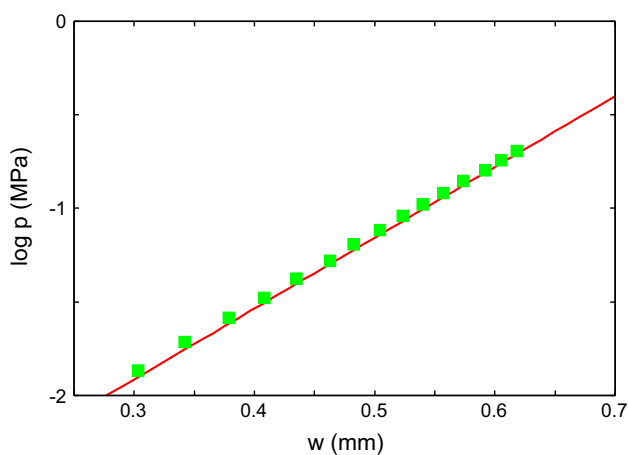


**Fig. 6** The relation between the natural logarithm of the nominal squeezing pressure,  $\log p$ , (in MPa) and the penetration  $w$  (in mm) obtained from experiment (green data points) for a rubber block in contact with a concrete road surface, and from the theory (red line). In the calculation, we used the measured  $h_{\max} = 1.49$  mm, the effective Young's modulus  $E_{\text{eff}} = 50$  MPa, and Poisson ratio  $\nu = 0.5$

surface as in Fig. 4) exhibits much larger (diameter  $\sim 5$  mm or less) macroasperity contact regions with larger average separations. But even in the latter case, the diameter of the contact regions is smaller than the rubber block thickness which is 10 mm.

#### 4 Comparing Experimental Data with Theory

We now compare the measured results with the theory predictions for 28 different road surfaces. Figure 6 shows the relation between the natural logarithm of the nominal squeezing pressure,  $\log p$  (in MPa), and the penetration  $w$  (in mm) obtained from experiment (green data points) and from

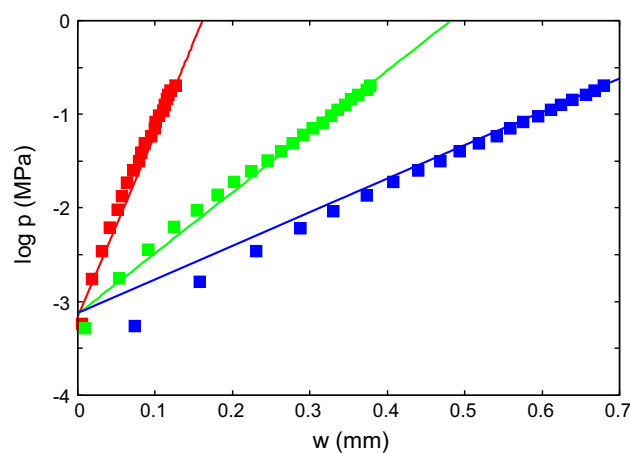


**Fig. 7** The relation between the natural logarithm of the nominal squeezing pressure,  $\log p$ , (in MPa) and the penetration  $w$  (in mm) obtained from experiment (square data points) for a rubber block in contact with three road surfaces, and from the theory (solid lines)

the theory (red line), for a rubber block in contact with a concrete road surface. In the calculation, we used the measured surface roughness power spectrum shown in Fig. 2, and  $h_{\max} = 1.49$  mm and the effective Young's modulus<sup>2</sup>  $E_{\text{eff}} = 50$  MPa and Poisson ratio  $\nu = 0.5$ . In this case, very good agreement prevails both for the slope of the linear

<sup>2</sup> The filled rubber compound we use exhibits strain softening with an elastic modulus which decreases from  $\approx 12$  MPa to  $\approx 4$  MPa as the strain increases from 0.1 to 10 %. The rubber strain in the asperity contact regions is approximately independent of the nominal contact pressure and relative large so the large strain  $E$ -module is most relevant and we take  $E \approx 4$  MPa. The effective modulus for the confined rubber disk is approximately given by the equation derived by Gent and Lindley (see Ref. [16]):  $E_{\text{eff}} \approx E(1 + 2S^2)$  where  $S = D/4d \approx 2.5$  (where  $D \approx 10$  cm is the diameter of the disk and  $d = 1$  cm the thickness of the disk). Thus, we get  $E_{\text{eff}} \approx 13.5E \approx 54$  MPa.

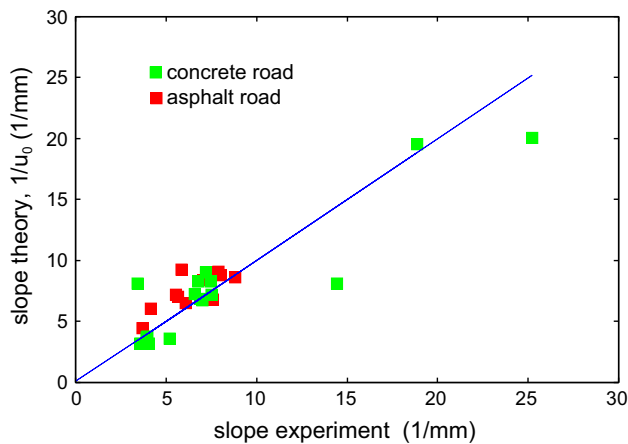


**Fig. 8** The calculated slope (equal to  $1/u_0$ ) (y-axis) of the relation between  $\log p$  and  $-\bar{u}$  as a function of the corresponding measured slope (x-axis). The blue line is given by  $y = x$

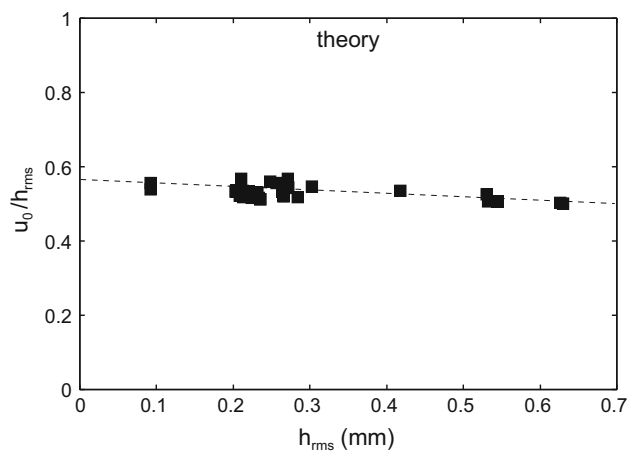


**Fig. 9** The ratio (theory)  $u_0/h_{rms}$  as a function of the root-mean-square roughness  $h_{rms}$  of the road surface

relation between  $\log p$  and  $w$  and the location of the line. In most other cases, there are some differences both for the slope and the position. Here, we will mainly focus on the slope of the line which determines the contact stiffness.

Figure 7 shows the same as in Fig. 6 but for three other road surfaces with very different rms roughness. It is interesting to note that for  $w = 0$  the straight lines converge to  $\log p \approx -3$  or  $p \approx 0.05$  MPa.

Figure 8 shows the calculated slope (equal to  $1/u_0$ ) of the relation between  $\log p$  and  $-\bar{u}$  as a function of the corresponding measured slope for all 28 substrate surfaces. The theoretical slopes were calculated using (5) with the measured surface roughness power spectrum as input.

Figure 9 shows the theoretical calculated ratio  $u_0/h_{rms}$  as a function of the root-mean-square roughness  $h_{rms}$  of the road surfaces. Note that this ratio is close to 0.5, but decreases slightly with increasing  $h_{rms}$ . This does not just

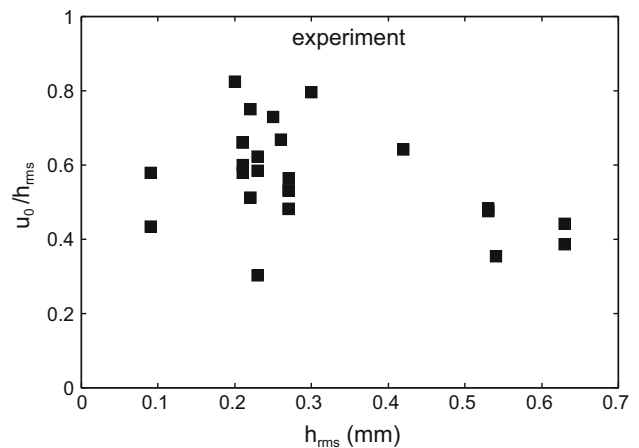


**Fig. 10** The ratio (experiment)  $u_0/h_{rms}$  as a function of the root-mean-square roughness  $h_{rms}$  of the road surface

reflect the increase in  $h_{rms}$  because one can show from (5) and (7) that scaling the power spectrum with a factor  $\lambda$  changes both  $u_0$  and  $h_{rms}$  by a factor  $\lambda^{1/2}$  so that the ratio is unchanged. Thus, the trend must reflect some (small) change in the shape of the surface roughness power spectrum  $C(q)$  as  $h_{rms}$  increases.

Figure 10 shows the same as in Fig. 9 but now with  $u_0$  deduced from the experiments. It appears that also in this case, there may be a small reduction in  $u_0/h_{rms}$  with increasing  $h_{rms}$ . The average of  $u_0/h_{rms}$  for all measured surfaces is  $0.56 \pm 0.13$  which is close to the average of the theoretical calculated data in Fig. 9 which is  $0.53 \pm 0.02$  (where  $\pm 0.02$  is  $\pm$  the standard deviation).

## 5 Summary and Conclusion

We have studied the relation between the nominal contact pressure  $p$  and the penetration  $w$  as an elastic solid (rubber block) is squeezed against randomly rough surfaces (asphalt and concrete road surfaces). In agreement with theory, in a large pressure range, the penetration is linearly related to  $\log p$ . The contact stiffness can be written as  $K = p/u_0$  where  $u_0$  is a length of order the rms roughness amplitude. For 28 different road surfaces, we have compared the theory prediction for  $u_0$  (which according to the theory is determined by the surface roughness power spectrum) with the values deduced from the measured relation between  $\log p$  and  $w$ . We find a good correlation between measured and calculated results. The presented results are relevant for several related problems such as heat transfer, contact resistance, damping of vibrations in mechanical contacts and some type of wear.

**Acknowledgments** The work underlying this report was commissioned by the Federal Ministry of Transport, Building and Housing under FE SV.0003/2009, by the Federal Ministry of Economics and Technology under 19 S 11002 and on behalf of the German Research Foundation. We thank Stephan Westermann (Goodyear, Luxemburg) and Boris Lorenz for comments on the manuscript.

## References

- Barber, J.R.: Bounds on the electrical resistance between contacting elastic rough bodies. *Proc. R. Soc. Lond. Ser. A* **459**, 53 (2003)
- Persson, B.N.J., Lorenz, B., Volokitin, A.I.: Heat transfer between elastic solids with randomly rough surfaces. *Eur. Phys. J. E* **31**, 3 (2010)
- Campana, C., Persson, B.N.J., Müser, M.H.: Transverse and normal interfacial stiffness of solids with randomly rough surfaces. *J. Phys. Condens. Matter* **23**, 085001 (2011)
- The data analyzed in this paper were presented before in: Wang, D., Ueckermann, A., Schacht, A., Oeser, M., Steinauer, B.: Relationship between the tire penetration depth and the road surface texture: a theoretical model and the practical application. In: *Proceeding of International Conference GeoHubei 2014*. However, the power spectra used in this reference was not accurate, and the results and conclusions obtained in the paper cited above are not accurate
- Persson, B.N.J.: Relation between interfacial separation and load: a general theory of contact mechanics. *Phys. Rev. Lett.* **99**, 125502 (2007)
- Yang, C., Persson, B.N.J.: Contact mechanics: contact area and interfacial separation from small contact to full contact. *J. Phys. Condens. Matter* **20**, 215214 (2008)
- Lorenz, B., Persson, B.N.J.: Interfacial separation between elastic solids with randomly rough surfaces: comparison of experiment with theory. *J. Phys. Condens. Matter* **21**, 015003 (2009)
- Lorenz, B., Carbone, G., Schulze, C.: Average separation between a rough surface and a rubber block: comparison between theories and experiments. *Wear* **268**, 984 (2010)
- Almqvist, A., Campana, C., Prodanov, N., Persson, B.N.J.: Interfacial separation between elastic solids with randomly rough surfaces: comparison between theory and numerical techniques. *J. Mech. Phys. Solids* **59**, 2355 (2011)
- Pastewka, L., Prodanov, N., Lorenz, B., Müser, M.H., Robbins, M.O., Persson, B.N.J.: Finite-size effect in the interfacial stiffness of rough elastic contacts. *Phys. Rev. E* **87**, 062809 (2013)
- Akarapu, S., Sharp, T., Robbins, M.O.: Stiffness of contacts between rough surfaces. *Phys. Rev. Lett.* **106**, 204301 (2011)
- Gäbel, G., Kröger, M.: *Proceedings of the INTER-NOISE 2007, Istanbul* (2007)
- Gäbel, G., Moldenhauer, P., Kröger, M.: Local effects between the tyre and the road. *ATZ* 0612008 **110**, 71 (2008)
- Gäbel, G.: *Beobachtung und Modellierung lokaler Phänomene im Reifen-Fahrbahn-Kontakt*. PhD thesis, University of Hannover (2009)
- Dapp, W.B., Prodanov, N., Müser, M.H.: Systematic analysis of perssons contact mechanics theory of randomly rough elastic surfaces. *J. Phys. Condens. Matter* **26**, 355002 (2014)
- Anderson, M.L., Mott, P.H., Roland, C.M.: The compression of bonded rubber disks. *Rubber Chem. Technol.* **77**, 293 (2004)
- Lyashenko, I.A., Pastewka, L., Persson, B.N.J.: On the validity of the method of reduction of dimensionality: area of contact, average interfacial separation and contact stiffness. *Tribol. Lett.* **52**, 223 (2013)
- Pohrt, R., Popov, V.L., Filippov, A.E.: Normal contact stiffness of elastic solids with fractal rough surfaces for one- and three-dimensional systems. *Phys. Rev. E* **86**, 026710 (2012)
- Barber, J.R.: Incremental stiffness and electrical contact conductance in the contact of rough finite bodies. *Phys. Rev. E* **87**, 013203 (2013)
- Persson, B.N.J., Albohr, O., Tartaglino, U., Volokitin, A.I., Tosatti, E.: On the nature of surface roughness with application to contact mechanics, sealing, rubber friction and adhesion. *J. Phys. Condens. Matter* **17**, R1 (2005)
- Persson, B.N.J.: On the fractal dimension of rough surfaces. *Tribol. Lett.* **54**, 99 (2014)
- Persson, B.N.J.: Contact mechanics for randomly rough surfaces. *Surf. Sci. Rep.* **61**, 201 (2006)
- Carbone, G., Mangialardi, L.: Analysis of the adhesive contact of confined layers by using a Green's function approach. *J. Mech. Phys. Solids* **56**, 684 (2008)
- Carbone, G., Lorenz, B., Persson, B.N.J., Wohlers, A.: Contact mechanics and rubber friction for randomly rough surfaces with anisotropic statistical properties. *Eur. Phys. J. E* **29**, 275 (2009)
- Persson, B.N.J.: *J. Phys.*: Contact mechanics for layered materials with randomly rough surfaces. *Condens. Matter* **24**, 095008 (2012)